Physical properties of the complex metallic alloy phases in the Al-Pd-Mn system

Janez Dolinsek, Zvonko Jaglicic, Ana Smontara

Physical properties of the complex metallic alloy phases in the Al-Pd-Mn system

Journal:	*Philosophical Magazine & Philosophical Magazine Letters*
Manuscript ID:	TPHM-05-Feb-0056.R2
Journal Selection:	Philosophical Magazine
Date Submitted by the Author:	26-Jul-2005
Complete List of Authors:	Dolinsek, Janez; J. Stefan Institute, F5 Jaglicic, Zvonko; Institute of Mathematics, Physics and Mechanics Smontara, Ana; Institute of Physics
Keywords:	transport properties, thermoelectric power, magnetic properties, aluminium alloys
Keywords (user supplied):	Complex metallic Alloys, Physical properties, Al-Pd-Mn system

Physical properties of the complex metallic alloy phases in the Al-Pd-Mn system

J. Dolinšek [1], Z. Jagličić [2], A. Smontara [3]

[1] *J. Stefan Institute, University of Ljubljana, Jamova 39, SI-1000 Ljubljana, Slovenia*

[2] *Institute of Mathematics, Physics and Mechanics, Jadranska 19, SI-1000 Ljubljana, Slovenia*

[3] *Institute of Physics, Bijenička 46, POB 304, HR-10001 Zagreb, Croatia*

The Al-Pd-Mn system of intermetallics contains complex metallic alloy (CMA) phases, whose crystal structures are based on giant unit cells comprising up to more than a thousand atoms per cell. We performed investigation of the magnetic, electrical, thermal transport and thermoelectric properties of the ξ' phase and the related Ψ phase on single-crystalline samples.

Short title: CMA phases in Al-Pd-Mn system

Keywords: Complex metallic alloys, Physical properties, Al-Pd-Mn system

I. INTRODUCTION

"Complex Metallic Alloys" (CMAs) [1,2] denote intermetallic phases whose giant unit cells with lattice parameters of several nanometers contain from many tens up to more than a thousand atoms. Inside the giant unit cells the atoms are arranged in clusters with polytetrahedral local atomic order of icosahedral or decagonal symmetry as typically found in quasicrystals (QCs). Consequently, in CMAs there exist two substantially different physical length scales—one defined by the cluster substructure and the other by the unit-cell parameters—so that interesting physical properties may appear from the competition between these different length scales.

Among the CMA materials, an interesting family of related structures was revealed in the Al-Pd alloys system [3,4] and its ternaries with transition metals (Mn, Fe, Co, Rh) [5-9]. The simplest regular structure discovered first in the Al-Pd-Mn [5,6] system, designated as ξ', contains 320 atoms in its orthorhombic unit cell. Some physical properties of single-crystalline samples of this compound grown by the self-flux technique were already reported [10]. Recently, centimeter-size single crystals of the ξ' phase and the related Ψ phase (containing about 1500 atoms in the unit cell) with the composition $Al_{74}Pd_{22}Mn_4$ were successfully grown using the Bridgman technique [11]. Here we present a study of their magnetic, electrical, thermal transport and thermoelectric properties.

II. SAMPLE PREPARATION

The sample materials were grown by the Bridgman technique, for details see [11]. Three samples were investigated under nominally the same experimental conditions. The samples were selected on the basis of previous TEM examinations [11]. Two

samples were cut from the same ingot and consisted of the major ξ' phase (referred to as the samples ξ'-AlPdMn-1 and ξ'-AlPdMn-2), whereas the third sample, of the major Ψ phase (referred to as Ψ-AlPdMn), was from another batch. The samples were shaped in the form of rectangular prisms with the long axis along the [0 1 0] direction. The backscattered electron (BSE) images of all three samples confirmed that the samples are single-phase crystals with no inclusion of secondary phases. The chemical composition of the samples was determined using energy-dispersive x-ray spectroscopy (EDXS) to be $Al_{73}Pd_{22.9}Mn_{4.1}$ for the ξ'-AlPdMn-1, $Al_{72.7}Pd_{23.2}Mn_{4.1}$ for the ξ'-AlPdMn-2 and $Al_{72.9}Pd_{22.9}Mn_{4.2}$ for the Ψ-AlPdMn, with the uncertainty ±0.5 for each element.

III. MAGNETIC MEASUREMENTS

The magnetization as a function of the magnetic field, $M(H)$, and the temperature-dependent magnetic susceptibility, $\chi(T)$, were measured with a Quantum Design SQUID magnetometer, equipped with a 5 T magnet. The susceptibility χ was investigated in the temperature interval between 300 and 2 K in a magnetic field H = 5 kOe applied along [010] direction (Fig. 1a). In this field the $M(H)$ dependence is linear (Fig. 1b), so we analyze $\chi = M/H$ in the following. The $\chi(T)$ values of all three samples are negative for the whole of the investigated temperature interval, indicating a dominant diamagnetic contribution. In addition, small paramagnetic Curie-like growth of the magnetization upon cooling is observed. The $\chi(T)$ data were analyzed by the sum of a Curie term and a temperature-independent term χ_0

$$\chi = \frac{C}{T-\theta} + \chi_0 , \qquad (1)$$

and the fits are shown as solid lines in Fig. 1a. The values of the parameters C (the Curie constant), θ (the Curie-Weiss temperature) and χ_0 are summarized in Table 1. For an electrically conducting material one generally expects three contributions of comparable size to the temperature-independent term χ_0: the negative Larmor diamagnetic contribution due to closed-shell ion cores, the negative Landau diamagnetic contribution due to orbital motion of conduction electrons in a magnetic field and the positive Pauli spin paramagnetic contribution due to conduction electrons, $\chi_0 = \chi_{Larmor} + \chi_{Landau} + \chi_{Pauli}$. The core contribution χ_{Larmor} can be estimated from Pascal tables [12]. For different choices of the ionization states of the elements (e.g. Mn^{2+}, Mn^{3+}, Mn^{4+}, Pd^{3+}, Pd^{4+},…) the calculated χ_{Larmor} values are all in the range between -0.6×10^{-3} and -0.8×10^{-3} *emu/mol*, whereas the experimental χ_0 values are in the interval between -0.5×10^{-3} and -0.6×10^{-3} *emu/mol*. We, therefore, have $\chi_0 \approx \chi_{Larmor}$, so that the diamagnetic contribution of the closed atomic shells dominates the temperature-independent term of the susceptibility. The small, negative values of the Curie-Weiss temperature θ should be considered as additional fit parameters only, which slightly improve the fits in Fig. 1a. No other experimental results suggest any antiferromagnetic interaction between the magnetic moments. The dominant diamagnetic behaviour is also observed in the $M(H)$ curves (Fig. 1b) obtained at 5 K, which exhibit a typical diamagnetic linear decrease with increasing H.

The Curie-type dependence of the paramagnetic part of the magnetization indicates the presence of localized magnetic moments in the structure. In analogy to *i*-Al-Pd-Mn QCs, it is straightforward to attribute this magnetization to the Mn species.

The small paramagnetic susceptibility, which even at 2 K is smaller than the diamagnetic core susceptibility, indicates that only a tiny fraction of the Mn atoms are magnetic. The fraction of magnetic moments in the samples can be estimated from the values of the Curie constant C, assuming that the magnetic manganese atoms are in the Mn^{2+} state with the effective Bohr magneton number $p_{eff} = 5.9$. The mean effective Bohr magneton number (the mean p_{eff} of all the Mn atoms in the sample) is calculated by using the formula [12] $\overline{p}_{eff} = 2.83\sqrt{C}$, which in turn yields the magnetic fraction as $f = \left(\overline{p}_{eff} / p_{eff}\right)^2$. The estimated f values of the three investigated samples are given in Table 1. They are very small and of comparable magnitude, all close to 1×10^{-4}. As the level of extrinsic magnetic impurities in the samples is of the order 10^{-5}, the measured magnetization contains both the Mn and the impurity moments. Therefore, the f values from Table 1 should be considered as an upper limit for the magnetic Mn fractions in the investigated samples. Similar small magnetic fraction (1 Mn out of every 60 000) and the conclusion on the significant contribution of impurity moments to the Curie magnetization was obtained also for the ξ' flux-grown monocrystals of composition $Al_{72}Pd_{25}Mn_3$ studied by Swenson *et al.* [10]. Comparing magnetic properties of the ξ' and Ψ samples to those of the *i*-Al-Pd-Mn QCs, the QCs are generally substantially more magnetic, with the magnetic Mn fractions typically one to two orders of magnitude larger [13], $f \approx 10^{-3} - 10^{-2}$.

IV. ELECTRICAL RESISTIVITY

The electrical resistivity $\rho(T)$ was determined in the temperature interval between 300 and 4 K using the standard four-terminal technique. The resistivity was measured along [0 1 0] direction of the samples and the data are displayed in Fig. 2. The room-temperature values are $\rho_{300K} = 213\ \mu\Omega cm$ for the ξ'-AlPdMn-1 sample, $\rho_{300K} = 192\ \mu\Omega cm$ for the ξ'-AlPdMn-2 and $\rho_{300K} = 229\ \mu\Omega cm$ for the Ψ-AlPdMn. These values are almost the same as those reported previously for the composition $Al_{72}Pd_{25}Mn_3$ [10]. The remarkable feature is the very small temperature variation of the resistivity in all three samples: $R = (\rho_{300K} - \rho_{4K})/\rho_{300K} = 1.4\ \%$ for the ξ'-AlPdMn-1, R = 0.5 % for the ξ'-AlPdMn-2, and R = 1.7 % for the Ψ-AlPdMn. Such a nearly temperature-compensated resistivity represents an intermediate case between the positive-temperature-coefficient (PTC) resistivity of metals (originating from the scattering of conduction electrons by phonons) and the negative-temperature-coefficient (NTC) resistivity commonly found in metallic glasses and QCs (due to a gradual electron localization caused by disorder/quasiperiodicity upon cooling). Relating the resistivities of the investigated ξ' and Ψ phases to those of the *i*-Al-Pd-Mn QCs, the ρ values of icosahedral samples are one order of magnitude larger (ranging typically from 1000 up to 4000 $\mu\Omega cm$). The $\rho(T)$ of the *i*-Al-Pd-Mn QCs is also drastically different. The resistivities of QCs usually exhibit negative temperature coefficients, but the magnitude of the NTC varies considerably between samples. In addition, the $\rho(T)$ of *i*-Al-Pd-Mn QCs in many cases displays a maximum between room temperature and 4 K and sometimes also a minimum at still lower temperatures.

V. THERMAL CONDUCTIVITY

The thermal conductivities were measured between 8 and 300 K along [010] direction using an absolute steady-state heat-flow method. The thermal flux through the samples was generated by a $1\ k\Omega$ RuO_2 chip-resistor, glued to one end of the sample, while the other end was attached to a copper heat sink. The temperature gradient across the sample was monitored by a chromel-constantan differential thermocouple. The temperature dependence of the thermal conductivity parameter $\kappa(T)$ of all three samples is displayed in Fig. 3. The $\kappa(T)$ values at 280 K are 8.6 *W/mK* for the ξ'-AlPdMn-1 sample, 7.3 *W/mK* for the ξ'-AlPdMn-2 and 5.0 *W/mK* for the Ψ-AlPdMn. These low $\kappa(T)$ values are of the same order as those of *i*-Al-Pd-Mn QCs [14], where they are considered to be a consequence of both the low electronic density of states (DOS) at the Fermi energy E_F and the nonperiodicity of the lattice, making the electronic and lattice contributions to the heat transport small. The thermal conductivity parameter $\kappa(T)$ is a sum of the electronic and lattice contributions, $\kappa = \kappa_{el} + \kappa_l$. The electronic contribution κ_{el} can be estimated using the Wiedemann-Franz law, $\kappa_{el} = L_0 T/\rho$ (where L_0 is the Lorenz number), and the measured electrical resistivity $\rho(T)$ data from Fig. 2. Due to the very small temperature dependence of $\rho(T)$ that enters the Wiedemann-Franz law, the electronic contribution $\kappa_{el}(T)$ exhibits practically linear temperature dependence (Fig. 3). Estimating the electronic contribution at 280 K we find, for the ξ'-AlPdMn-1, $\kappa_{el} = 3.3\ W/mK$, wherefrom we get the lattice contribution $\kappa_l = \kappa - \kappa_{el} = 5.3\ W/mK$ with the ratio $\kappa_{el}/\kappa_l = 0.62$. For the ξ'-AlPdMn-2 we get $\kappa_{el} = 3.6\ W/mK$, $\kappa_l = 3.7\ W/mK$ and $\kappa_{el}/\kappa_l = 0.97$, whereas for the Ψ-AlPdMn we get $\kappa_{el} = 3.0\ W/mK$,

$\kappa_l = 2.0\ W/mK$ and the ratio $\kappa_{el}/\kappa_l = 1.5$. For all three samples, κ_{el} and κ_l are thus of comparable size at room temperature. This is different from both simple metals, where the electronic contribution is usually 1–2 orders of magnitude larger than the lattice contribution, and Al-based QCs, where electrons carry less than 1 % of the heat.

VI. THERMOELECTRIC POWER

The thermopower measurements were performed at temperatures between 300 and 4 K by applying a differential method with two identical thermocouples (chromel–gold with 0.07 % iron), attached to the sample with silver paint. The thermoelectric power data (the Seebeck coefficient $S(T)$) are shown in Fig. 4. The thermopowers of all three investigated samples are negative across the whole investigated temperature interval, indicating that electrons are the dominant charge carriers. The room-temperature S values are rather small, ranging between –4.7 and –8 $\mu V/K$. While the ξ'-AlPdMn-1 and ξ'-AlPdMn-2 samples exhibit a relatively smooth temperature variation of $S(T)$, the thermopower of the Ψ-AlPdMn sample shows a strong (absolute) increase between 4 K and 8 K, followed by a weaker increase at higher temperatures. For all samples, $S(T)$ shows several changes of slope within the investigated temperature range.

VII. CONCLUSIONS

We investigated magnetic, electrical, thermal transport and thermoelectric properties of the giant-unit-cell ξ' and Ψ CMA phases in the Al-Pd-Mn system. Magnetic susceptibility measurements have shown that the samples are diamagnets with a tiny paramagnetic Curie-like magnetization. The estimated fraction of magnetic Mn atoms

(assumed to be in the Mn^{2+} state) in all samples is about 1×10^{-4}. The electrical resistivity amounts about $200\ \mu\Omega cm$ and is temperature-independent to within less than 2 % in the investigated interval between 300 and 4 K. The thermal conductivity of the ξ' and Ψ samples is small, comparable in magnitude to that of *i*-Al-Pd-Mn QCs. This suggests that a low electronic DOS at the E_F and a low phonon density are at the origin of the weak heat transport in the ξ'-Al-Pd-Mn CMAs. The thermoelectric power of about $-6\ \mu V/K$ at room temperature is small, compatible with a low concentration of charge carriers, and negative, indicating that electrons are the majority carriers.

Acknowledgement: We thank M. Feuerbacher for provision of the samples.

Table 1: Parameters C, θ and χ_0 obtained from the fits of the temperature-dependent magnetic susceptibility. The magnetic fraction f of Mn atoms was calculated from the Curie constants C, assuming the atoms are in the Mn^{2+} state ($p_{eff} = 5.9$).

sample	C (emu K)/mol Mn	θ (K)	χ_0 ($\times 10^{-3}$ emu/mol sample)	f
ξ'-AlPdMn-1	3.0×10^{-3}	-3.0	-0.59	0.7×10^{-4}
ξ'-AlPdMn-2	4.7×10^{-3}	-3.2	-0.56	1.0×10^{-4}
Ψ-AlPdMn	6.9×10^{-3}	-5.4	-0.52	1.6×10^{-4}

References:

[1] The term "Structurally Complex Alloy Phases" or SCAPs is also sometimes used in literature.

[2] See, for a recent review, K. Urban and M. Feuerbacher, J. Non-Cryst. Solids **334&335**, 143 (2004).

[3] Y. Matsuo, K. Hiraga, Phil. Mag. Lett. **70**, 155 (1994).

[4] M. Yurechko, A. Fattah, T. Velikanova, B. Grushko. J. Alloys Comp. **329**, 173 (2001).

[5] M. Boudard, H. Klein, M. de Boissieu, M. Audier, H. Vincent, Philos. Mag. A **74**, 939 (1996).

[6] H. Klein, M. Audier, M. Boudard, M. de Boissieu, L. Behara, M. Duneau, Philos. Mag. A **73**, 309 (1996).

[7] S. Balanetskyy, B. Grushko, T. Ya. Velikanova, K. Urban, J. Alloys Comp. **376**, 158 (2004).

[8] M. Yurechko, B. Grushko, T. Velikanova, K. Urban, J. Alloys Comp. **337**, 172 (2002).

[9] S. Balanetskyy, B. Grushko, T. Ya. Velikanova, Z. Kristall. **219**, 548 (2004).

[10] C. A. Swenson, I. R. Fisher, N. E. Anderson, Jr., P. C. Canfield, A. Migliori, Phys. Rev. B **65**, 184206 (2002).

[11] M. Feuerbacher, C. Thomas, K. Urban, in *Quasicrystals, Structure and Physical Properties*, Ed. H.-R. Trebin (Wiley-VCH, Weinheim, 2003), p. 2.

[12] F. E. Mabbs, D. J. Machin, *Magnetism and Transition Metal Complexes* (Chapman and Hall, London, 1973), p. 7.

[13] F. Hippert, M. Audier, J. J. Préjean, A. Sulpice, E. Lhotel, V. Simonet, Y. Calvayrac, Phys. Rev. B **68**, 134402 (2003).

[14] A. Bilušić, Ž. Budrović, A. Smontara, J. Dolinšek, P. C. Canfield, I. R. Fisher, J. Alloys. Compd. **342**, 413 (2002).

Figure captions:

Fig. 1: (a) Temperature-dependent magnetic susceptibility χ in a field $H = 5$ kOe (solid lines are fits described in the text) and **(b)** magnetization M as a function of the magnetic field H at $T = 5$ K (the slight nonlinearity in the vicinity of $H = 0$ is due to a thin ferromagnetic surface oxide layer). The dashed lines serve as a guide for the eye and "f. u." denotes "formula unit" (e.g. one $Al_{73}Pd_{22.9}Mn_{4.1}$ unit in the case of ξ'-AlPdMn-1 sample).

Fig. 2: Temperature-dependent electrical resistivities.

Fig. 3: Temperature-dependent thermal conductivities $\kappa(T)$ between 8 and 300 K. Squares, circles and triangles represent the total conductivities, whereas the dotted, dashed and dash-dot lines represent the electronic contribution κ_{el}, estimated from the Wiedemann-Franz law.

Fig. 4: Thermoelectric power $S(T)$ between 4 and 300 K.

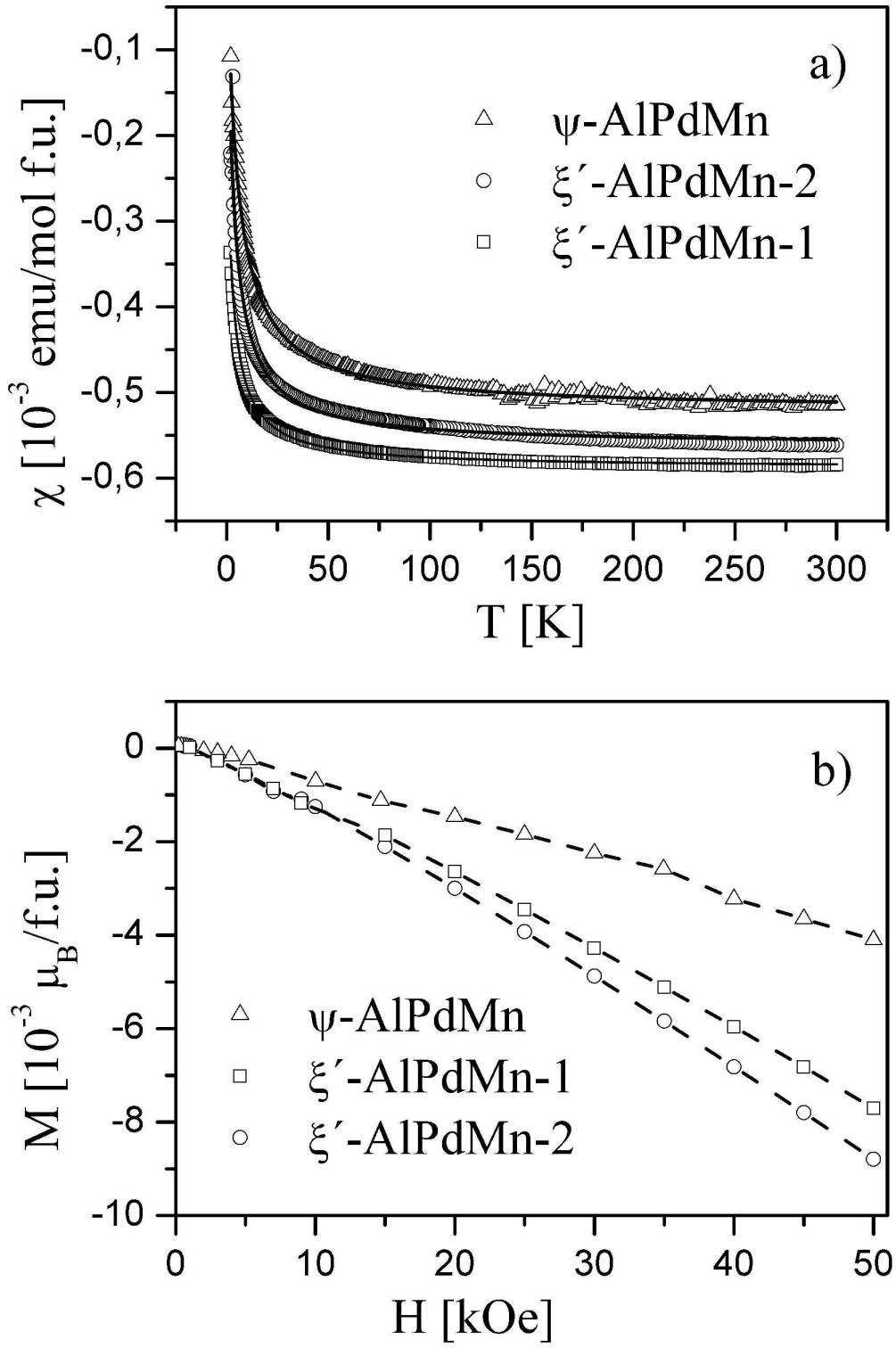
a)
ψ-AlPdMn
ξ´-AlPdMn-2
ξ´-AlPdMn-1
χ [10^-3 emu/mol f.u.]
T [K]
b)
ψ-AlPdMn
ξ´-AlPdMn-1
ξ´-AlPdMn-2
M [10^-3 μB/f.u.]
H [kOe]

Fig. 1

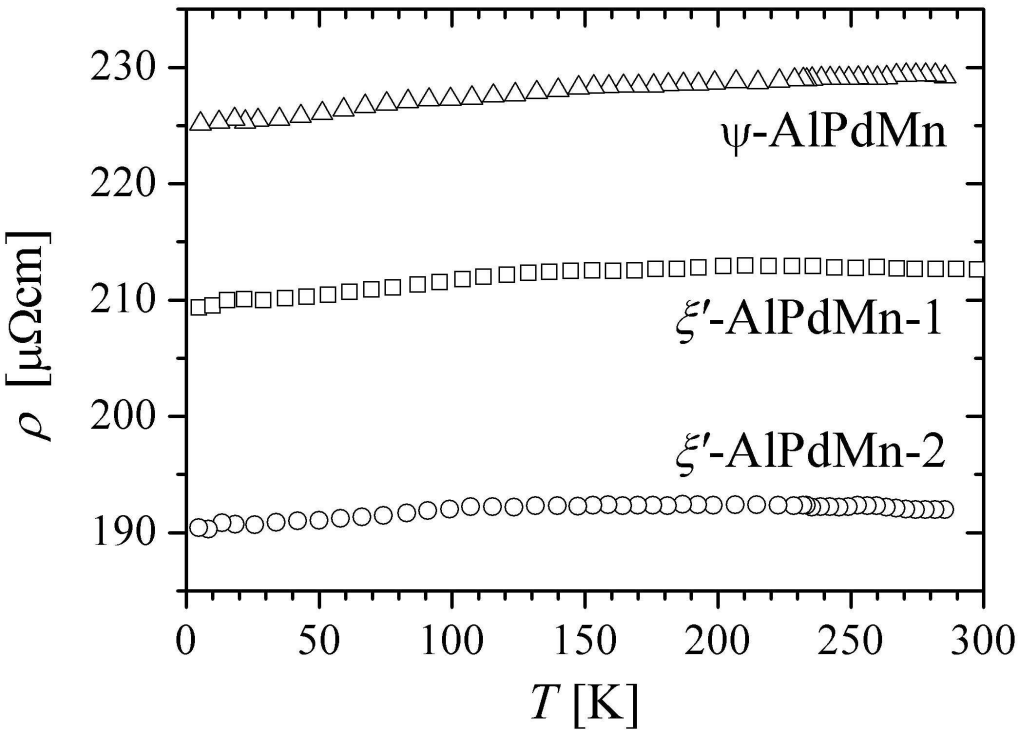

Fig. 2

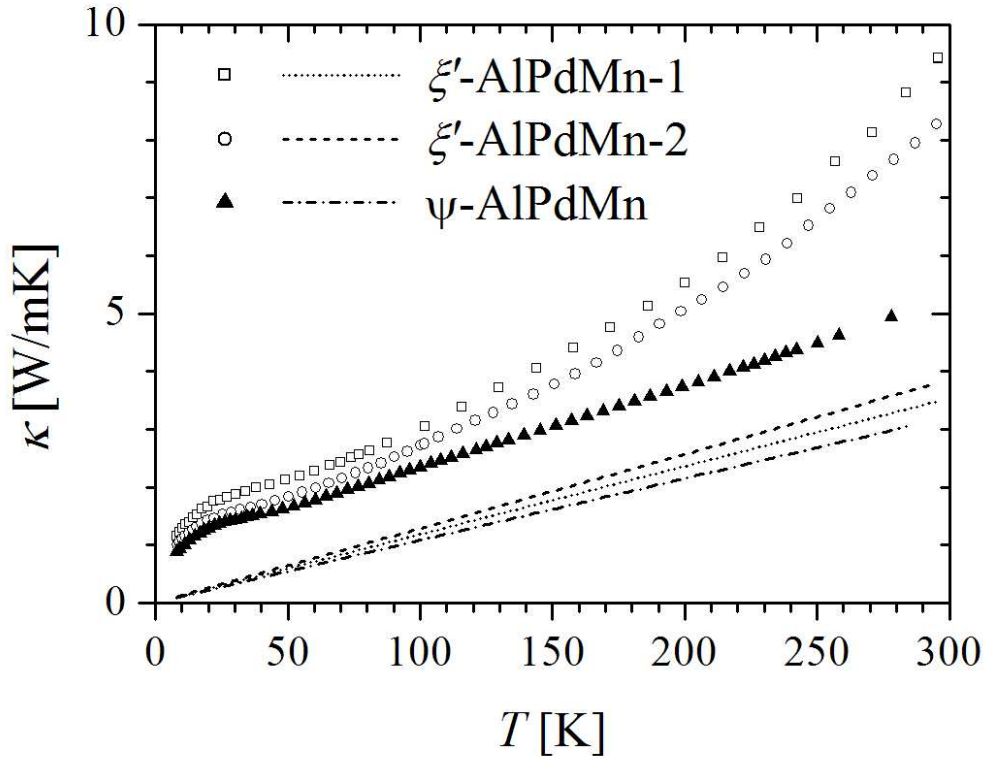
10
5
0
0
50
100
150
200
250
300
κ [W/mK]
T [K]
ξ′-AlPdMn-1
ξ′-AlPdMn-2
ψ-AlPdMn

Fig. 3

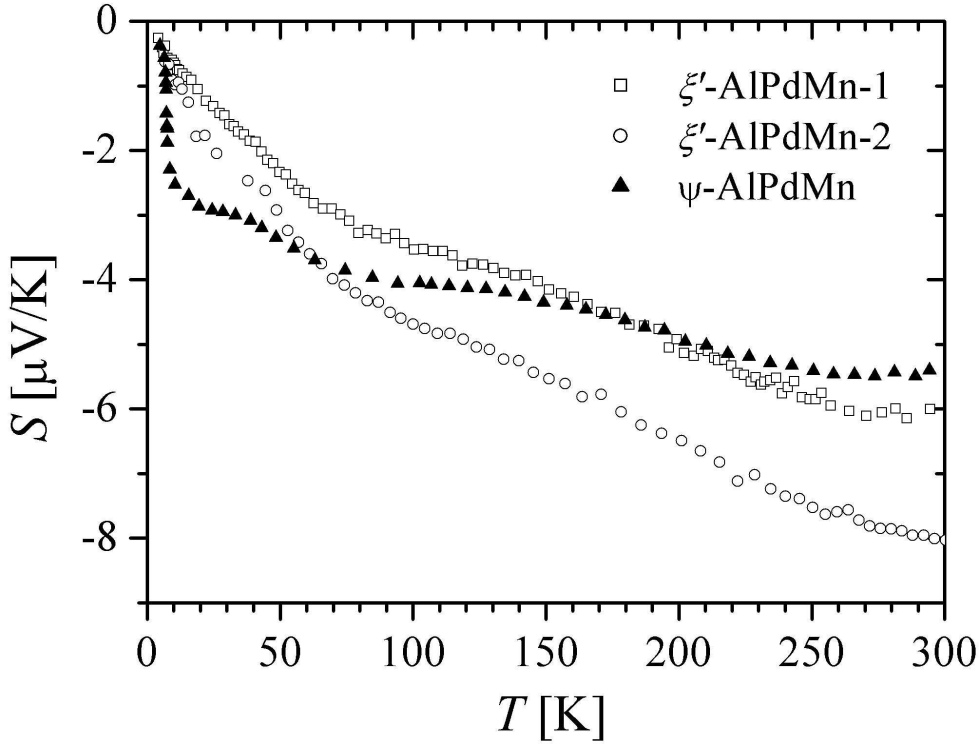

Fig. 4